Two Thermoeconomic Diagnosis Methods Applied to Representative Operating Data of a Commercial Transcritical Refrigeration Plant

Ommen, Torben Schmidt; Sigthorsson, Oskar; Elmegaard, Brian

Published in:
Entropy

Link to article, DOI:
10.3390/e19020069

Publication date:
2017

Document Version
Publisher's PDF, also known as Version of record

entropy

MDPI

Article

Two Thermoeconomic Diagnosis Methods Applied to Representative Operating Data of a Commercial Transcritical Refrigeration Plant

Torben Ommen *, Oskar Sigthorsson † and Brian Elmegaard

Department of Mechanical Engineering, Technical University of Denmark, 2800 Kongens Lyngby, Denmark; oskarsig@gmail.com (O.S.); be@mek.dtu.dk (B.E.)

* Correspondence: tsom@mek.dtu.dk; Tel.: +45-45-25-40-37

† Current address: Marorka, 105 Reykjavik, Iceland

Academic Editor: Vittorio Verda

Received: 20 December 2016; Accepted: 8 February 2017; Published: 15 February 2017

Abstract: In order to investigate options for improving the maintenance protocol of commercial refrigeration plants, two thermoeconomic diagnosis methods were evaluated on a state-of-the-art refrigeration plant. A common relative indicator was proposed for the two methods in order to directly compare the quality of malfunction identification. Both methods were applicable to locate and categorise the malfunctions when using steady state data without measurement uncertainties. By introduction of measurement uncertainty, the categorisation of malfunctions became increasingly difficult, though depending on the magnitude of the uncertainties. Two different uncertainty scenarios were evaluated, as the use of repeated measurements yields a lower magnitude of uncertainty. The two methods show similar performance in the presented study for both of the considered measurement uncertainty scenarios. However, only in the low measurement uncertainty scenario, both methods are applicable to locate the causes of the malfunctions. For both the scenarios an outlier limit was found, which determines if it was possible to reject a high relative indicator based on measurement uncertainty. For high uncertainties, the threshold value of the relative indicator was 35, whereas for low uncertainties one of the methods resulted in a threshold at 8. Additionally, the contribution of different measuring instruments to the relative indicator in two central components was analysed. It shows that the contribution was component dependent.

Keywords: refrigeration; exergy; thermoeconomic diagnosis; measurement uncertainty

1. Introduction

The use of refrigeration equipment is a major energy consumer on global scale, with estimates as high as 17.2% in terms of electricity consumption [1] and additional consumption shares based on thermal supply. With such a share, even small improvements in the average performance may prove highly beneficial in order to limit operation cost, increase security of supply, and constrain the environmental concerns related to power consumption.

With currently used maintenance protocols, operation anomalies are often detected and located at fixed service intervals. This implies that malfunctioning components can remain in use for very long periods of time. If a more comprehensive method was used for detecting and identifying malfunctions, it would result in significant energy savings on both local and global level, as well as possible cost reductions, if energy savings outweighs the additional maintenance [2].

The primary objectives of the thermoeconomic diagnosis approaches are to locate and categorise malfunctions at component level, and to quantify their effects on the system performance. In general,

the considered malfunctions are due to operation anomalies, which cause a decreased efficiency of the system, and thus more resources are required in order to obtain the same product.

Malfunctions can be categorised into external, intrinsic and induced malfunctions [3]. The intrinsic malfunctions are the actual causes of malfunctions. The external malfunctions are due to altered conditions outside the system boundary and do not represent degraded components. External malfunctions may be conceived as off-design operation with corresponding change in component operational conditions. The intrinsic and external malfunctions may induce apparent malfunctions in other components, as the operation conditions may no longer correspond to the expected design or off-design operating condition. Although apparently malfunctioning, components subject to induced malfunctions are not subject to operation anomalies. This is especially important for vapour compression cycles as "*any fault will propagate to the whole plant*" [4].

Using simple diagnosis methods, the indication of all three types of malfunctions are typically similar. This has lead to large interest in rule-based fault detection and diagnosis, which is utilised to identify any intrinsic anomaly [5–7]. Although applicable to locate and categorise the anomaly, rule-based fault detection has not been successfully implemented in the refrigeration industry, due to the complex and time-consuming methods that should be applied for each plant individually.

Focus on the use of thermoeconomic diagnosis approaches have increased in the refrigeration community within the last couple of years [8,9]. Previously, the method was mainly applied to complex thermal systems with large production capacities such as power generation [10]. However, the concept of thermoeconomic diagnosis was extended to the field of refrigeration early on, although with limited interest to "*provide results of particular interest from an engineering point of view*" [11]. A particular finding of d'Accadia and de Rossi [11] is the presence of several dissipative components and the "*concept of negentropy*". This topic is further addressed in later scientific literature regarding thermoeconomic analysis of refrigeration plants [12–16].

Two previously presented methods to locate and categorise malfunctions are of particular interest. The two methods are:

A. Characteristic curve method [17,18].
B. Thermoeconomic model diagnosis approach [19,20].

Both methods have been introduced and used in the TADEUS (thermoeconomic approach to the diagnosis of energy utility systems) test case [21,22], which is a steady state combined cycle power plant simulator. The diagnosis is based on numerical simulations of both design and off-design conditions. Specifically in Lazzaretto et al. [23], the two methods are recommended in terms of their applicability to locate the malfunctions and filter the induced effects. The effect of measured data on the thermoeconomic model diagnosis approach is considered by Verda and Borchiellini [24]. This is done by evaluating the uncertainty of measured data, and later to include the derived uncertainty of measurements in the diagnosis. The evaluation of uncertainties is considered in steady state conditions. In a paper by Usón et al. [25] the operation of a power plant is presented using thermoeconomic diagnosis for a period of more than six years. Silva et al. [26] suggest a prognosis method to "*indicate the plant performance gain*", as a post-processing of the characteristic curves method, or a similar method to locate and categorize anomalies.

In the present study, the thermoeconomic diagnosis approach is proposed as the method to identify malfunctions on component level, using already installed equipment. The hypothesis is, that thermoeconomic diagnosis can assist in reducing the delay between the start of the operation anomaly and the moment in which it is detected by the operator of the system. By determining options of corrective actions, the operator may further be able to perform an economic optimisation. With efficient replacement or repair of the degraded component (once the operation anomaly is detected and located), the malfunctioning components experience reduced operation time with a lowered efficiency, thus reducing the overall electricity consumption. Another benefit of efficient maintenance is the possibility of meeting the full, dimensioned capacity at all times, thereby either improving the

security of supply of cold production or allowing for a corresponding down-scale of the refrigeration plant. The considered system is a small commercial refrigeration plant, where many thermodynamic variables are measured and logged at high frequency.

The objective of this paper is to evaluate the applicability of the two thermoeconomic diagnosis methods to locate and categorise malfunctions in a commercial refrigeration plant for a supermarket, based on a steady state thermodynamic model of the plant, even when measurement uncertainty of representative data is included. Two uncertainty scenarios are considered to represent the full uncertainty of measurement equipment according to it's data sheet, as well as an estimated scenario, where uncertainties are based only on hysteresis and repeatability of the equipment. A focus of the study is also to evaluate whether the use of the already existing measuring instruments in the system is applicable for further work, or if some of the measuring instruments should be changed or located elsewhere. A quantification of the effects of malfunctions, as well as an economic optimal corrective action, is not examined in the present study.

By assessing the applicability of the two methods and the current equipment to perform diagnosis, the paper focuses on the possible pending integration in smaller applications and at temperatures closer to ambient, which may be of particular interest from an engineering or development point of view.

2. Method

A calculation procedure for the application of the two thermoeconomic diagnosis methods using measured data is presented in Figure 1a, considering the case where the behaviour of the components is known. Two calculations are required in order to perform the diagnosis: determination of exergy flows (reconciliation) and the actual thermoeconomic diagnosis calculation.

In the present analysis, a numerical model was used to substitute real operation data, as knowledge of the location of the intrinsic malfunction was required to compare and verify the result of the diagnosis method. In this case, measurement uncertainties were added to each of the used thermodynamic quantities.

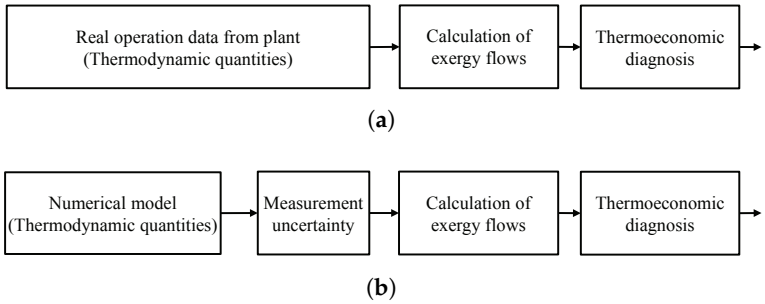

Figure 1. Procedure to perform diagnosis based on measured data or from numerical model. (**a**) Measured data; (**b**) Data from numerical model with added measurement uncertainty.

The procedure to perform diagnosis based on data from a numerical model is presented in Figure 1b. The numerical operations are:

- A model is developed in order to obtain steady state thermodynamic quantities (T, p, $\dot{m}$ and electricity consumption, as discussed later) of the refrigeration system without measurement uncertainties.
- Measurement uncertainty is added to the measured thermodynamic quantities.
- Another simulation model is required to calculate the exergy flows of the individual streams simulating a real case where only the measured thermodynamic quantities in the actual plant are known.
- The two investigated thermoeconomic diagnosis methods are applied individually for the considered components.

The individual parts of the calculation procedure are further discussed in Sections 2.1–2.3. Information of the measurement uncertainty is presented in Section 2.4.

Both of the considered methods require additional operating conditions in a number of different operating points in order to model the behaviour of the components, i.e., in terms of the characteristic curves and the thermoeconomic models. The models should be developed prior to the actual diagnosis evaluation. The models can be based on thermodynamic quantities, either from measured data or from a numerical model of the plant [18,24].

In order to derive the models which describe the behaviour of the components, measured thermodynamic quantities were considered. This is at the same time the case where the largest influence of measurement uncertainty was found to occur. Using this method, both the developed models and the diagnosis was exposed to measurement uncertainty. A schematic illustration of the complete calculation procedure is presented in Figure 2.

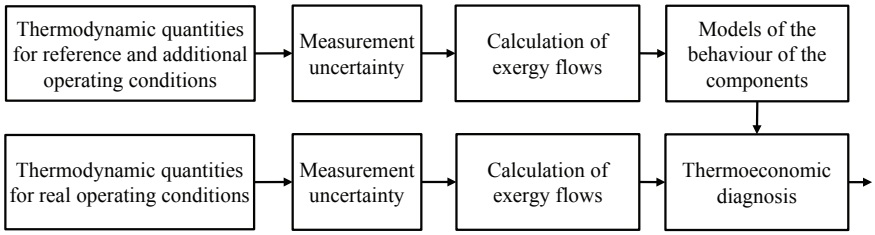

Figure 2. Schematic representation of the calculation procedure to evaluate the impact of measurement uncertainty on the indication of malfunctions in refrigeration plant.

As an alternative, the approximations for a real plant could be derived directly from a numerical model. In this case the approximations of behaviour of the components would not be affected by measurement uncertainty, but subject to any inconsistency between the numerical model and the actual plant operation. The accuracy of such a solution is considered a subject of further investigation, as the incomplete representation may cause erroneous categorisation of malfunctions.

All of the addressed models were developed and interconnected in the numerical tool EES V9.710 [27].

2.1. Numerical Model

The conceptual design of commercial refrigeration plants for a supermarket is different from country to country mainly due to differences in legislation and climate. In Denmark, most newly built refrigeration plants are designed much like the one previously presented in literature [8,28]. The refrigerant is Carbon Dioxide (R744). The refrigerant is a natural refrigerant with low Global Warming Potential (GWP). A schematic representation of the system including state points and instrumentation is shown in Figure 3.

The acronyms used in the figure represent the main components in the refrigeration cycle: one High Pressure compressor unit (HP), one Low Pressure compressor unit (LP), a Gas Cooler unit (GC), several Chilled Temperature evaporator units (CT) and several Freezing Temperature evaporator units (FT). The system is scalable to meet refrigeration demands of both large and small commercial applications. The system configuration in smaller supermarkets is as presented in Figure 3 with two compressors for each stage. The two compressors for each stage are dimensioned for different flow rates. Depending on investment cost, electricity prices and impact on durability, frequency converters are applicable on both compressor stages [29]. The GC fan and HP compressors are operated in order to minimise total electricity consumption.

In order to evaluate the use of thermoeconomic diagnosis in refrigeration, a numerical model of a transcritical booster refrigeration plant was developed. A similar model is presented in [8]. The purpose of the model was to supply the data needed to substitute measured data from the

refrigeration plant. Temperature, pressure and mass flow of each state point were calculated. The use of a numerical model proposes transparency for the reader, easy repeatability and the possibility to obtain steady state thermodynamic data. A representative *T*–*s* diagram is presented in Figure 4.

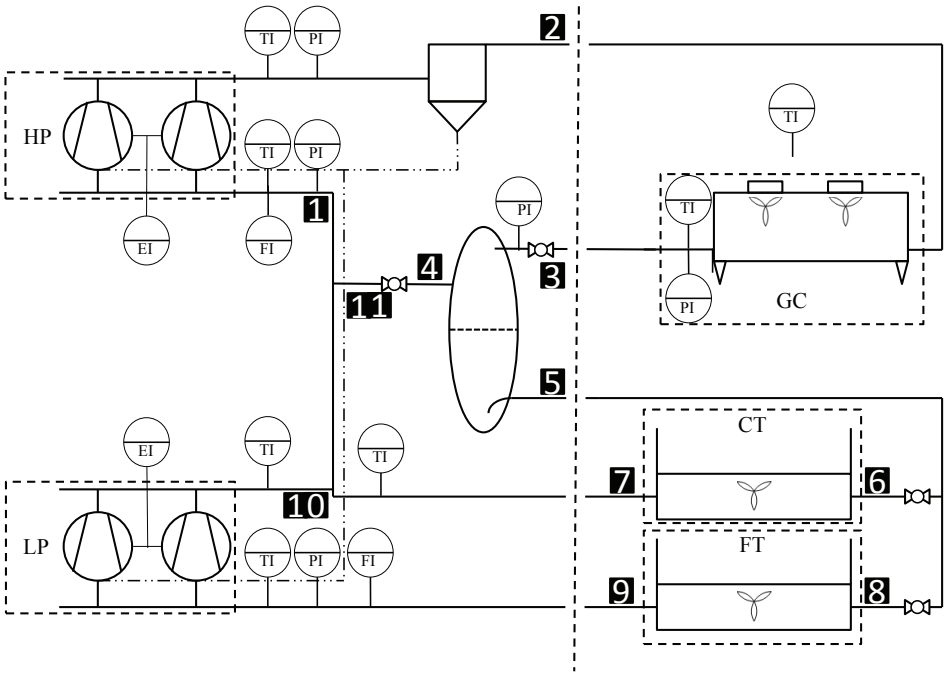

Figure 3. Schematic diagram of the transcritical refrigeration plant with control volumes for five main components. State points are shown in black squares. Instrumentation for measured quantities are presented with following notation: TI—temperature; PI—pressure; FI—Flow and EI—electrical consumption.

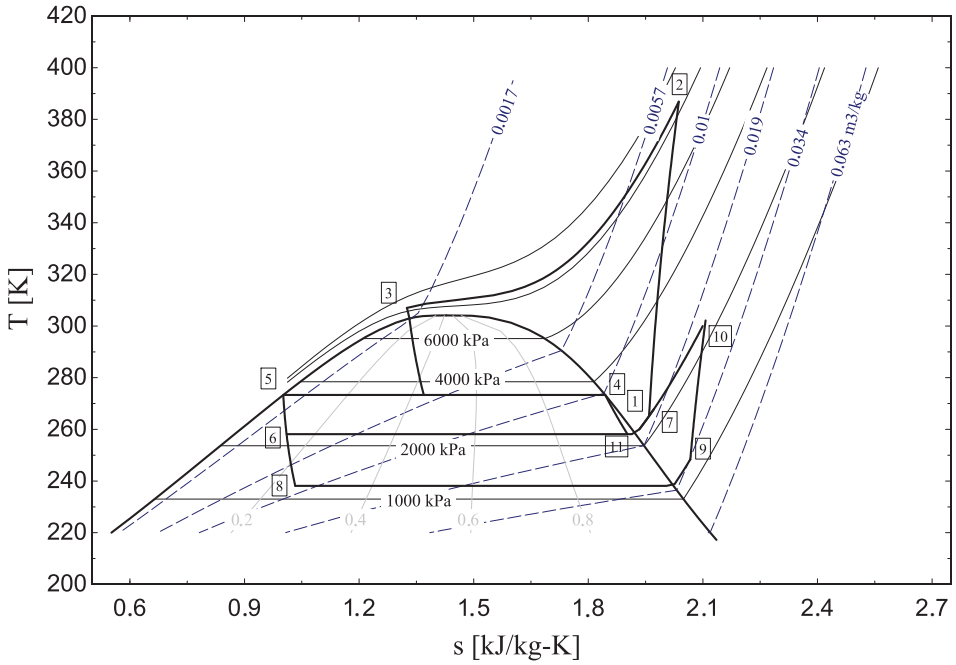

Figure 4. Representative temperature–entropy diagram of refrigerant R744 (CO2) and a transcritical booster refrigeration plant with state points according to Figure 3 [8].

Minor changes were implemented in the model, compared to the previously published one. The intention of these revisions was to more closely represent the temperatures, pressures and mass flow rates of the actual plant. The parameters of the utilised model are presented in Table 1. The use of coherent state variables between the numerical model and the measurements ensures coherency between the exergy flows in the individual state points and the measurement uncertainties.

Table 1. Estimated thermodynamic parameters used in the numerical refrigeration plant model.

Parameter	Value	Unit	Description
η_{HP}	0.7	/	HP isentropic efficiency (including η_{el})
$\dot{Q}_{HP}$	0	kW	HP heat loss to oil separator and pipes
η_{LP}	0.7	/	LP isentropic efficiency (including η_{el})
$\dot{Q}_{LP}$	0	kW	LP heat loss to oil separator and pipes
t_{GC}	32	°C	Temperature of air entering the Gas Cooler
UA_{GC}	8.1	kW/K	Overall conductance in Gas Cooler (sum of discretised model)
p_{HP}	0	kPa	Pressure loss in Gas Cooler
$\dot{W}_{GC,fan}$	1.52	kW	Rated fan power in Gas Cooler
$\dot{m}_{GC,fan}$	4.72	kg/s	Mass flow of air in Gas Cooler at rated power
p_{3-4-5}	3500	kPa	Intermediate pressure in liquid receiver
$\dot{Q}_{CT}$	24	kW	Refrigeration load of combined store at CT temperature
UA_{CT}	2.7	kW/K	Conductance in CT evaporator
$t_{SH,CT}$	10	K	Superheat of refrigerant in CT
p_{CT}	0	kPa	Pressure loss in CT
$\dot{W}_{CT,fan}$	1	kW	Rated fan power in CT
$t_{CT,in}$	−5	°C	Temperature of air after CT evaporator
$t_{CT,out}$	3	°C	Temperature of air prior to CT evaporator
$\dot{Q}_{FT}$	15	kW	Refrigeration load of combined store at FT temperature
UA_{FT}	0.7	kW/K	Conductance in FT evaporator
$t_{SH,FT}$	10	K	Superheat of refrigerant in FT
p_{FT}	0	kPa	Pressure loss in FT
$\dot{W}_{FT,fan}$	1	kW	Rated fan power in FT
$t_{FT,in}$	−25	°C	Temperature of air after FT evaporator
$t_{FT,out}$	−18	°C	Temperature of air prior to FT evaporator

The temperature of the refrigerant leaving the GC was assumed closely linked to the operation scheme of the combined refrigeration plant. The use of available experimental data for the numerical model resulted in a discretised heat exchanger model of the GC. The UA value presented in Table 1 represents the total heat transfer area of the discretised model.

2.2. Calculation of Exergy Flows

Besides needed equipment for safety requirements outlined by local legislation, the refrigeration plant is equipped with several temperature indicators and pressure gauges, used for commissioning, regulation and maintenance of the system. The performed work focused on the use of already installed measuring instruments, as promising results may be directly implemented in supermarkets, where equivalent dimensioning and structure was used, or will be used, during commissioning.

To accommodate the above consideration, a separate model was developed to evaluate the exergy flow of each stream based the on thermodynamic quantities from the schematics of the refrigeration system, with the measured variables presented in Figure 3. Only measured quantities were allowed as input to the model, as this resembles the way experimental data would be used to perform the thermoeconomic diagnosis. In the evaluation of the exergy flows, only the physical component was considered, as the chemical composition of the individual streams was assumed constant.

The model for reconciliation of measured quantities was primarily based on energy and mass balances at component level, along with simple assumptions of the refrigerant quality in the evaporators and the receiver.

Thermodynamic quantities for temperature and pressure were used as input parameters. Regarding the mass flows of refrigerant, applicable instrumentations are typically not available in newly commissioned plants. The use of flow instrumentation is possible, although typically not utilised in practise. In the analysis, two flow instruments were considered in the superheated vapour preceding the compressor racks. The requirements in terms of measurement uncertainty for flow instrumentation is further addressed in Sections 2.4 and 3.3. The electricity consumption was monitored for both compressor racks. Additional variables were measured for the different evaporators, but due to the investigation detail at component level, further instrumentation was not needed for the presented analysis.

2.3. Thermoeconomic Diagnosis Methods

In the study at hand, exergy and exergoeconomic analysis was based on the formulation as presented by Bejan et al. [30]. This choice implied some minor cosmetic changes in the formulation of the two methods, which are presented in Sections 2.3.1 and 2.3.2. Additionally, to achieve a more convenient comparison of the two methods in the present study, the derivations of a common relative indicator is presented in Section 2.3.3.

The characteristic curve method and the thermoeconomic model diagnosis approach have been proposed, analysed and discussed in several papers. The analysis performed in this study, rely mainly on the formulation in [18,24], respectively.

2.3.1. Characteristic Curve Method

The characteristic curves approach is based on knowledge of the complex dependency of the thermodynamic variables of streams entering and exiting a component [18]. The dependencies are characterised based on the units commissioning in a reference condition, or are determined from a representative model. The distinctive differences between intrinsic and induced malfunction are found by comparing real operating data (where an anomaly may be present), to a prediction of the effects of an induced malfunction.

To evaluate an anomaly, a dependent variable was calculated for both the examined condition as well as the induced operation. Component irreversibility in terms of exergy destruction rate was chosen as the dependent variable, as this variable describes the component behaviour [18]. Another reason for choosing exergy destruction as dependent variable, is that the quantity is always positive and lowest in the case of no anomaly.

The difference between the two dependent variables was calculated as presented in Equation (1).

$$I^i = \Delta\dot{E}_D^i - \Delta\dot{E}_{D,\text{calc}}^i = \Delta\dot{E}_D^i - \left(\sum_k \left[\frac{\delta\dot{E}_D^i}{\delta\tau_k^i}\right]_{\text{ref}} \Delta\tau_{k,\text{real}}^i\right) \quad (1)$$

where I^i is the indicator for the ith component, exergy destruction rate $\dot{E}_D$ as the dependent variable, ${}^{\delta\dot{E}_D^i}/_{\delta\tau_k^i}$ is the characteristic curve function, and τ_k is the kth independent variable.

In practice the calculated characteristic curves may be simplified linearisations of the the complex thermodynamic dependencies that occur for induced malfunctions. The usability of such simple linearisation depends on the characteristic behaviour as well as the close proximity of the reference point. Such simple characteristic curves may be approximated using a set of independent variables matching the degree of freedom in the component considered. The chosen independent variables were thermodynamic variables such as mass flow, temperature and refrigerant pressure. In order to achieve the characteristic curves, an amount of non-malfunctioning operating conditions must be found along

with a reference condition. The linearised system to solve is presented in Equation (2). The amount of operating conditions n must in this case match the degrees of freedom in the component m.

$$\begin{bmatrix} \Delta\tau_{1,1} & \Delta\tau_{1,2} & \cdots & \Delta\tau_{1,n} \\ \Delta\tau_{2,1} & \Delta\tau_{2,2} & \cdots & \Delta\tau_{2,n} \\ \vdots & \vdots & \ddots & \vdots \\ \Delta\tau_{m,1} & \Delta\tau_{m,2} & \cdots & \Delta\tau_{m,n} \end{bmatrix} \begin{bmatrix} \frac{\delta\dot{E}_D^i}{\delta\tau_1^i} \\ \frac{\delta\dot{E}_D^i}{\delta\tau_2^i} \\ \vdots \\ \frac{\delta\dot{E}_D^i}{\delta\tau_m^i} \end{bmatrix} = \begin{bmatrix} \Delta\dot{E}_{D,1} \\ \Delta\dot{E}_{D,2} \\ \vdots \\ \Delta\dot{E}_{D,n} \end{bmatrix} \tag{2}$$

2.3.2. Thermoeconomic Model Diagnosis Approach

The thermoeconomic model diagnosis approach relies on a productive structure, expressed in terms of exergy flows, to describe the physical structure [24]. As an alternative to the productive structure [31,32], the definitions introduced by Bejan et al. [30] can be used.

The identification between the intrinsic and induced malfunction was accomplished by a comparison between a "free" and the reference operating conditions. The "free" operating condition was calculated based on the real condition. This was done by modelling the behaviour of the component using the exergy product for each component as the dependent variable and the exergy fuel rate as the independent variable. To compare the two operating conditions, the expected exergy product rate at the reference operating condition was calculated. The exergy product rate from the real operating condition was linearly approximated back to the reference operating condition. "*If the anomalies are small enough, the (free) operating condition is quite close to the reference condition. In this case the effect of every adjustment parameter moved by the control system on the flows can be considered linear*" [24]. This is expressed for the ith component as:

$$\dot{E}_{P,\text{free}}^i = \dot{E}_{P,\text{real}}^i + \sum_k \left[\frac{\delta\dot{E}_P^i}{\delta\dot{E}_{F,k}}\right]_{\text{ref}} (\dot{E}_{F,k,\text{ref}}^i - \dot{E}_{F,k,\text{real}}^i) \tag{3}$$

where $E_{P,\text{free}}$ is the exergy flow of the product in the "free" operating condition, and derivatives ${}^{\delta\dot{E}_P^i}/_{\delta\dot{E}_{F,k}}$ are used to convert the real operating condition to the free condition.

In the formulation of the productive structure used by Verda and Borchiellini [24] the level of detail of the productive structure can be increased by splitting the physical exergy flows into thermal and mechanical components. However, limited improvement in the accuracy of the thermoeconomic diagnosis is gained [33].

To develop the derivatives additional operating condition were required, which are equal in number to the degrees of freedom, in the vicinity of the reference operating condition [24]. By following this method, the derivatives were obtained in similar fashion as those in Equation (2).

2.3.3. Common Indicator

For the thermoeconomic model diagnosis approach, the indication of malfunctions was changed to correspond closely to the indicator of the Characteristic curve method [3]. More precisely, the used indicator determines the difference between the exergy product rate and the expected exergy product rate at the reference operating condition. In case the expected exergy product rate is lower than the exergy product rate, an increased exergy destruction rate occurs in the component, and the difference is caused by an intrinsic malfunction. The indicator was formulated for the ith component as:

$$I^i = \Delta\dot{E}_D^i - \Delta\dot{E}_{D,\text{free}}^i = \Delta\dot{E}_D^i - (\dot{E}_{P,\text{ref}}^i - \dot{E}_{P,\text{free}}^i) \tag{4}$$

The indicator depends on the absolute exergy destruction rate in the component. In an evaluation of a complete plant operation, the use of a relative indicator might assist in locating the crucially

degraded components. The proposed relative indicator is defined for the *i*th component using the exergy destruction rate at the reference operating condition:

$$I^i_{\text{rel}} = \frac{I^i}{\dot{E}^i_{D,\text{ref}}} = \frac{\Delta\dot{E}^i_D - (\dot{E}^i_{P,\text{ref}} - \dot{E}^i_{P,\text{free}})}{\dot{E}^i_{D,\text{ref}}} \tag{5}$$

Identically, the relative indicator for the characteristic curve method can be revised to match the relative indicator defined in Equation (5):

$$I^i_{\text{rel}} = \frac{I^i}{\dot{E}^i_{D,\text{ref}}} = \frac{(\Delta\dot{E}^i_D - \Delta\dot{E}^i_{D,\text{calc}})}{\dot{E}^i_{D,\text{ref}}} \tag{6}$$

2.4. Measurement Uncertainty

When thermoeconomic diagnosis is applied to the refrigeration plant, both the reference and additional operating conditions to approximate the characteristic curves and the thermoeconomic models, will be based on data where measurement uncertainty may change the reading of the quantity. Therefore, the modelled behaviour of the components includes measurement uncertainty from the corresponding measuring instruments.

As the measurement of the thermodynamic quantities used to model the behaviour of the components was done by the same instruments repeatedly, special conditions may apply which for some equipment will decrease the uncertainty. Table 2 presents the measurement uncertainty of representative measurement equipment in a transcritical refrigeration plant. The instrument uncertainties were evaluated in two scenarios, denoted as "data sheet" and "estimated".

The "data sheet" scenario represents the full measurement uncertainty of the instrument according to its data sheet. The data was based on information from the instrument data-sheets (e.g., [34–36]). The measurement uncertainties of the flow instruments were based on estimations. However, as the measurement uncertainty from the flow instruments is important for the study at hand, the effect of the considered measurement uncertainty is further investigated in Section 3.3. The measurement uncertainty that was used to represent flow instruments in both of the cases considered in Table 2 was significantly higher than what is possible when using Coriolis flow meters (e.g., [37]).

Table 2. Measurement uncertainty of the evaluated measuring instruments in the two scenarios.

Measured Quantity	State Points	Absolute/Relative	Deviation (k = 2)		Unit
			Data Sheet	Estimated	
Temperature	All	Absolute	0.5	0.1	°C
Pressure (>5500 kPa)	2; 3	Absolute	128	16	kPa
Pressure (<5500 kPa)	1; 4; 9	Absolute	48	6	kPa
Mass flow of refrigerant	1; 9	Relative	2	1	%
Electricity consumption	1; 9	Relative	1.2	0.6	%

The use of the "data sheet" measurement uncertainty scenario does not take into consideration that the uncertainty of a measurement covers several different components related to the actual measuring instrument, out of which typically only a minor part of the uncertainty is measuring hysteresis and repeatability (e.g., [35,37]). The difference for only including a part of the measurement uncertainty was represented by the estimated case. For several of the instrumentation types used in the investigation, the individual uncertainty components, such as the contribution of hysteresis, are listed in the data-sheets. In the case where the approximations of the characteristic curves and the thermoeconomic models of the components are based on measured thermodynamic quantities, the approximations will correspondingly include the offset, such as linearity deviation and thermal zero point from the calibration of its measuring instruments [35].

As for the measurement uncertainties assumed in Table 2, the resulting uncertainty on the derived relative indicators was calculated using $k = 2$ (results shown with 95% confidence).

3. Results

A reference calculation was carried out to support the analysis and the results of the paper. Besides the reference conditions, four real operating conditions with malfunctions were considered, denoted as "real #":

1. Increased operation pressure in refrigerant receiver by 300 kPa.
2. Reduction in LP-compressor isentropic efficiency by 0.1 /.
3. Reduction in HP-compressor isentropic efficiency by 0.1 /.
4. Malfunctioning fan at air side of the Gas Cooler → mass flow of air reduced by 50%.

Finally, additional operating conditions were established by small variations in external parameters, in order to numerically compute the needed derivatives for the two methods.

Malfunctions were evaluated for the five main components of the refrigeration plant. The five components are marked with acronyms in Figure 3. The three latter real operating conditions include an intrinsic malfunction in one of the components under consideration. However, the first real operating condition only includes induced malfunctions in the components under consideration. No external malfunctions are included in the respective operating conditions.

The reference and real operating conditions of the refrigeration plant, according to the state points defined in Figure 3, are presented in Table A1 in Appendix A.

3.1. Evaluation of the Thermoeconomic Diagnosis Methods without Measurement Uncertainties

The initial evaluation was carried out using steady state data obtained from the numerical model of the refrigeration plant, without measurement uncertainties. This resembles the method presented in Figure 1a.

The obtained results are presented in Table 3 for both of the considered thermoeconomic diagnosis methods. Some of the partial calculation results are included, as this allows for a convenient comparison with the referenced papers [18,24]. In the sub-table to the far right of Table 3, the proposed common relative indicator is presented, with highlighted colour in the areas where intrinsic malfunctions should be present according to the respective operation anomalies.

The results showed, that both diagnosis methods were able to successfully identify the intrinsic malfunctions and filter out induced malfunctions, caused by intrinsic malfunctions in other components. Based on the small relative indicators for components with induced malfunctions it was found plausible, that the use of linearised models for the derivatives of the components was sufficient to identify the operation anomalies.

The relative indicators of components with intrinsic malfunctions in the different real operating conditions were of equal magnitude between the two methods considered. The differences of the relative indicators for components with induced malfunctions (especially in Real 1) were slightly increased considering method B.

Table 3. Calculation example without measurement uncertainties. For the proposed common relative indicator, the areas were highlighted where intrinsic malfunctions should be present according to the respective operation anomalies.

	Method A (Characteristic Curve Method [17,18])															
	$\dot{E}_D^i$ **(kW)**				$\Delta\dot{E}_{D,\mathrm{real}}^i$ **(kW)**				$\Delta\dot{E}_{D,\mathrm{calc}}^i$ **(kW)**				I_{rel}^i **[/]**			
	Real 1	**Real 2**	**Real 3**	**Real 4**	**Real 1**	**Real 2**	**Real 3**	**Real 4**	**Real 1**	**Real 2**	**Real 3**	**Real 4**	**Real 1**	**Real 2**	**Real 3**	**Real 4**
HP Comp	3.60	3.60	5.51	3.76	0.01	0.01	1.93	0.18	0.01	0.01	0.32	0.18	−0.1	0.0	44.6	−0.4
GC unit	5.51	5.57	6.16	5.93	0.00	0.05	0.65	0.41	0.00	0.07	0.78	4.74	0.1	0.2	1.6	43.5
CT unit	0.89	0.90	0.90	0.89	0.00	0.00	0.00	0.00	0.01	0.00	0.00	0.00	−1.1	0.0	0.0	0.0
FT unit	0.24	0.24	0.24	0.25	0.00	0.00	0.00	0.00	0.00	0.00	0.00	0.00	−1.0	0.0	0.0	0.0
LP Comp	0.28	0.42	0.27	0.27	0.01	0.15	0.00	0.00	0.01	0.03	0.00	0.00	0.7	43.5	0.0	0.0
	Method B (Thermoeconomic Model Diagnosis Approach [19,20])															
	$\dot{E}_{P,\mathrm{real}}^i$ **(kW)**				$\dot{E}_{P,\mathrm{free}}^i$ **(kW)**				$(\dot{E}_{P,\mathrm{ref}}^i - \dot{E}_{P,\mathrm{free}}^i)$ **(kW)**				I_{rel}^i **[/]**			
	Real 1	**Real 2**	**Real 3**	**Real 4**	**Real 1**	**Real 2**	**Real 3**	**Real 4**	**Real 1**	**Real 2**	**Real 3**	**Real 4**	**Real 1**	**Real 2**	**Real 3**	**Real 4**
HP Comp	45.3	45.3	45.9	46.8	45.2	45.2	43.7	45.2	0.00	0.00	1.48	−0.01	0.0	−0.1	41.3	−0.4
GC unit	39.9	39.7	39.7	40.9	39.7	39.7	39.7	41.7	0.00	0.00	0.00	2.04	0.0	0.0	0.0	37.0
CT unit	16.8	16.4	16.4	16.4	16.3	16.4	16.4	16.4	0.04	0.00	0.00	0.00	1.5	0.0	0.0	0.0
FT unit	3.5	3.4	3.4	3.4	3.4	3.4	3.4	3.4	0.01	0.00	0.00	0.00	0.9	0.0	0.0	0.0
LP Comp.	4.2	4.1	4.1	4.1	4.1	4.0	4.1	4.1	0.00	0.11	0.00	0.00	1.6	40.2	0.0	0.0

3.2. Evaluation of the Thermoeconomic Diagnosis Methods with Measurement Uncertainties

In order to include measurement uncertainty in the evaluation, the thermoeconomic diagnosis was recalculated with the new information. The plant data presented in the appendix is still applicable as the reference, but for the individual quantities uncertainty was included as presented in Figure 1b. Assumptions for the measuring instruments correspond to the uncertainties presented in Table 2. The impact of the measurement uncertainty is evaluated based on the previously presented results from Table 3, which in the following results are presented as the baseline result, from which the error bars are extended.

The effects of measurement uncertainties on the relative indicators are presented in Figures 5–8. Considering Figure 5, the results on the left hand side (Figure 5a) represents the data sheet scenario, while the results presented on the right hand side (Figure 5b) represents the estimated scenario. For each of the considered main components, the resulting uncertainty utilising both method A and B is presented. As an example, the results presented in Figure 5a correspond to the calculated baseline I^i_{rel} from Table 3, which were found to result in indicators of 0 ± 2 (only considering the induced malfunctions). Based on these results, the possible errors of the evaluation are indicated according to the measurement uncertainty of the data sheet scenario. Considering the HP compressor, the error bars show uncertainties of $u(I^i_{\mathrm{rel}}) = \pm 15$ for method A, and $u(I^i_{\mathrm{rel}}) = \pm 16$ for method B. For the GC unit, the error bars show uncertainties of $u(I^i_{\mathrm{rel}}) = \pm 33$ for method A, and $u(I^i_{\mathrm{rel}}) = \pm 13$ for method B. Hence, the significant uncertainties of the measurements results in very high variations of the malfunction indicator. Even negative values may appear. This may challenge the interpretation of the results.

For the estimated scenario (Figure 5b), the uncertainty of the calculated results was considerably lower. As an example, the error bars for the HP compressor show uncertainties of $u(I^i_{\mathrm{rel}}) = \pm 7$ for method A, and $u(I^i_{\mathrm{rel}}) = \pm 7$ for method B.

The Figures 6–8 show the effect of measurement uncertainties on the relative indicator for the remaining three real operating conditions. In each of the sub-figures, the results for both diagnosis methods are presented concurrently for each considered component. Four main deductions were drawn from the analysed cases (corresponding to Figures 5–8):

- Both methods were applicable to locate and categorise malfunctions for the estimated uncertainty measurement scenarios. For method B, a significant margin was present between induced and intrinsic malfunctions in all cases. The difference between highest possible induced result and lowest intrinsic result was found to be $\Delta I_{\mathrm{rel}} = 12$. For method A, the differences between induced and intrinsic malfunction of the relative indicator were slightly lower ($\Delta I_{\mathrm{rel}} = 9$).
- In the data sheet scenario, overlaps between the relative indicators for components with intrinsic and induced malfunctions were found, due to high measurement uncertainties. This was the case for both method A and B.
- The impact of the measurement uncertainty on the relative indicator was of equal magnitude for the two methods, considering both measurement uncertainty scenarios.
- For the data sheet scenario, a relative indicator above the value of $I_{\mathrm{rel}} = 35$ was found to indicate an intrinsic malfunction in the considered components. Using the estimated uncertainty scenario, the threshold value of the relative indicator for induced effects was approximately $I_{\mathrm{rel}} = 14$ for method A (the characteristic curve method), and $I_{\mathrm{rel}} = 8$ for method B (the thermoeconomic model diagnosis approach).

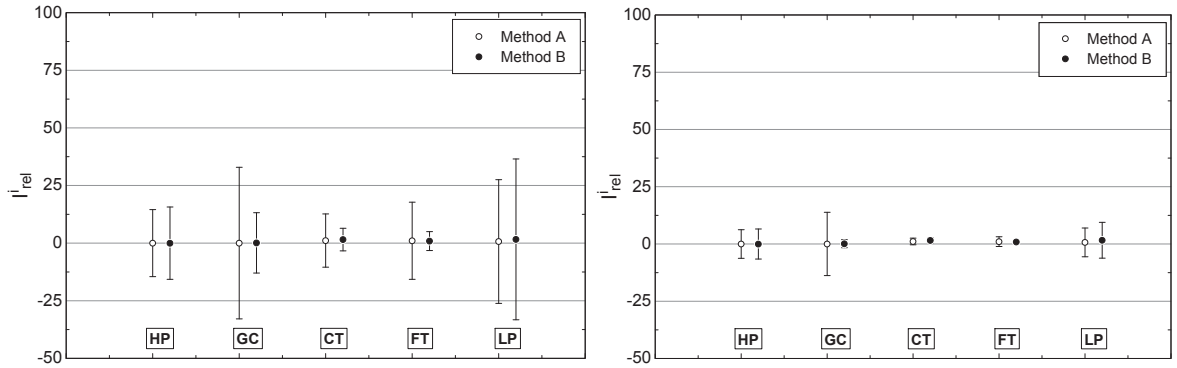

(**a**) (**b**)

Figure 5. The effect of measurement uncertainties on the proposed relative indicator for Real 1 with two different uncertainty scenarios. (**a**) Data sheet; (**b**) Estimated.

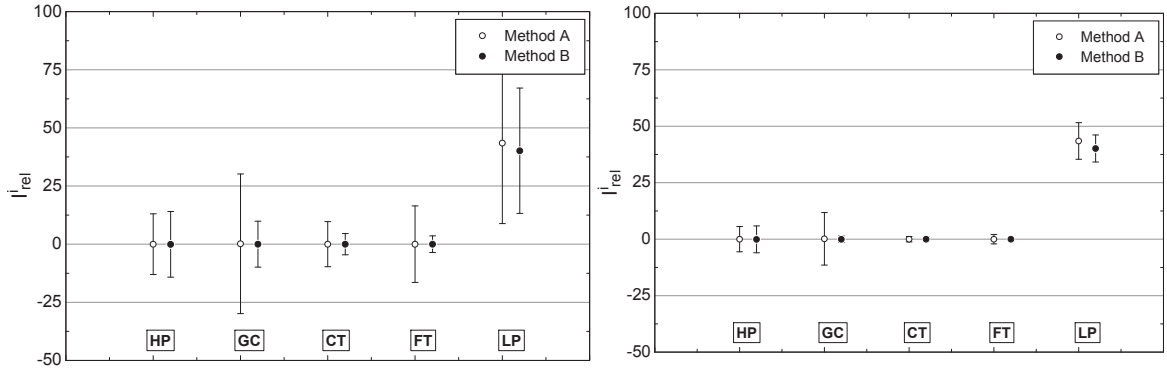

(**a**) (**b**)

Figure 6. The effect of measurement uncertainties on the proposed relative indicator for Real 2 with two different uncertainty scenarios. (**a**) Data sheet; (**b**) Estimated.

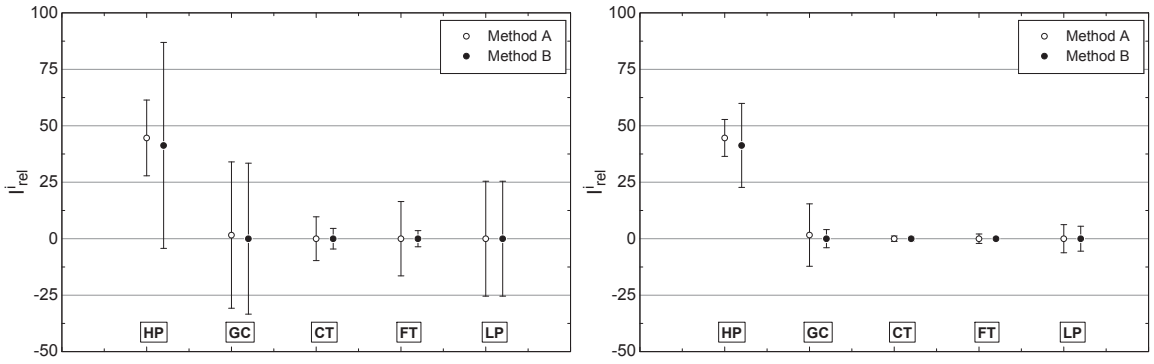

(**a**) (**b**)

Figure 7. The effect of measurement uncertainties on the proposed relative indicator for Real 3 with two different uncertainty scenarios. (**a**) Data sheet; (**b**) Estimated.

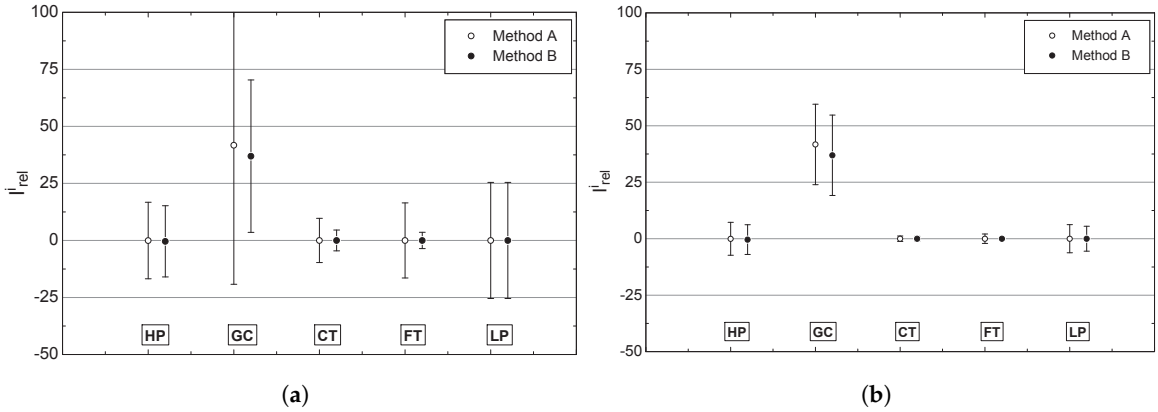

Figure 8. The effect of measurement uncertainties on the proposed relative indicator for Real 4 with two different uncertainty scenarios. (**a**) Data sheet; (**b**) Estimated.

3.3. Critical Measuring Instrument

According to the above results, measurement uncertainty was found to be a significant figure for the indicator. An assessment of the individual contributions to the combined uncertainty was deemed important to obtain reasonable quality when performing diagnosis. The assessment was performed for two components (HP and GC) using the characteristic curve method (method A).

The evaluation was based on a variation of the relative measurement uncertainty of the mass flow instruments between zero and data sheet scenario values. This was chosen as applicable instrumentations for flow measurements are typically not available in newly commissioned plants, and thus may present additional capital cost to the owner. The data sheet and estimated scenarios were used, for temperature and pressure transmitters, as well as electricity consumption, respectively. These were thus according to Table 2.

For the HP compressor, the contributions of measurement uncertainty from the related measuring instruments are presented in Figure 9. The results are presented for measurement uncertainty according to the data sheet scenario in Figure 9a, and for the estimated scenario in Figure 9b. The displayed curves represent the collected uncertainty of the specific instrument, e.g., all the used pressure readings were contained in one overall contribution. The four inputs to the diagnosis procedure (temperature, pressure, mass flow and electricity consumption) were normalised to present their relative impact on the combined uncertainty. The resulting uncertainty on the relative indicator $\pm u(I^i_{\text{rel}})$ is presented on the right hand ordinate axis. The resulting uncertainty corresponds to the uncertainty of the relative indicator used in Figures 5–8, e.g., the uncertainty of I^i_{rel} for relative uncertainty of flow measurement of 2% corresponds the the previously addressed uncertainty of $u(I^i_{\text{rel}}) = \pm 15$.

For low measurement uncertainties of the mass flow instrumentation (considering the data sheet scenario in Figure 9a), uncertainty from electricity and pressure measurement instruments are by far the major component in the comparison. With increasing relative measurement uncertainty of mass flow, the contribution of flow measurements is increased above the contribution of pressure measurements. In the considered range, the contribution from flow instrumentation is at maximum 65% of the combined uncertainty. For the estimated scenario (Figure 9b) electric consumption was found to be the significant contribution in case the relative mass flow measurements were below 0.6. Above this level mass flow measurements became increasingly important.

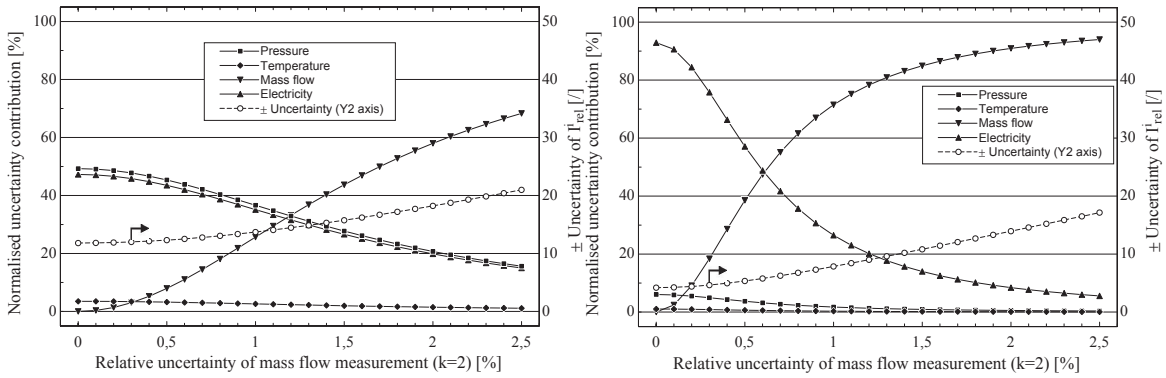

Figure 9. Evaluation of the individual contributions of measurement uncertainties for the HP compressor. Flow measurement uncertainty is varied from negligible to high relative uncertainties. The combined measurement uncertainty on the relative indicator $\pm u(I^i_{\mathrm{rel}})$ is presented on the right hand ordinate. (**a**) Data sheet; (**b**) Estimated.

For the Gas Cooler unit, a similar evaluation of the measurement uncertainty contribution was performed, which is presented in Figure 10. The main contribution of measurement uncertainty is from the various temperature measurements for both the data sheet scenario (Figure 10a) and the estimated scenario (Figure 10b). Even with high relative uncertainty of the mass flow of refrigerant, more than 95% of the uncertainty corresponds to temperature measurement using the data sheet scenario.

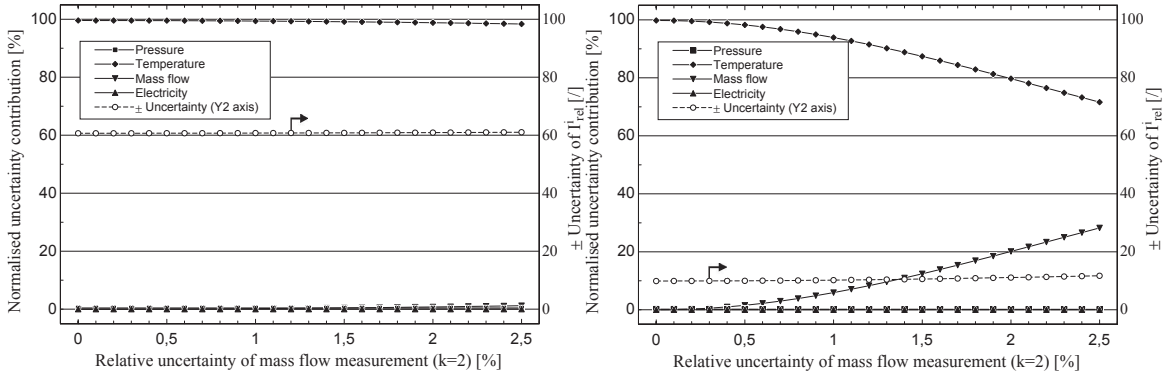

Figure 10. Evaluation of the individual contributions of measurement uncertainties for the Gas Cooler unit. Flow measurement uncertainty is varied from negligible to high relative uncertainties. The combined measurement uncertainty on the relative indicator $\pm u(I^i_{\mathrm{rel}})$ is presented on the second ordinate. (**a**) Data sheet; (**b**) Estimated.

It was found that Figures 9 and 10 showed clear differences in trends between the contributions of measurement uncertainty from the individual types of units investigated. According to the results in Section 3.2, pressure measurements were found not to provide a significant contribution to the overall measurement uncertainties. For the flow measurements, the difference between negligible flow measurement uncertainty and high uncertainty shows to change the overall uncertainty of I^i_{rel} less than 50%.

4. Discussion

The objective of the analysis was to evaluate the performance of two thermoeconomic diagnosis methods applied to a refrigeration plant where measurement uncertainty was included in the reference, additional and real operating conditions. From the results, it was possible to state an expected confidence in the quality of measured relative indicators in an equivalent commercial refrigeration plant, if the data were obtained from steady state operation. Both thermoeconomic diagnosis methods proved applicable with the measuring instruments considered in this study using the estimated uncertainty scenario.

The methods were found to be quite similar both in terms of derivation and the corresponding results. One key difference is the variables used for characterisation, where method A utilises thermodynamic variables, contrary to method B where thermoeconomic variables are used for the analysis. It was considered possible, that the differences between individual deviations for the relative indicator may depend on the characteristics due to nonlinear behaviour. The overall influence of measurement uncertainties was however not subject to such characteristics. It should be noted that achieving the maximum uncertainty in the relative indicator, shown by the uncertainty bars for both scenarios in Figures 5–8, is only possible if a number of measurements have experienced their maximal and converging measurement uncertainty ($k = 2$), in the thermoeconomic diagnosis procedure presented in Figure 2. With the possibility of repeated measurements a lower coverage factor could be used (e.g., $k = 1$). Another proposed method to evaluate the repeated measurement is to fix distribution functions for each quantity, and subsequently perform Monte Carlo simulation for the relative indicator.

Based on the analysis of the contribution of each measuring instrument on the measurement uncertainties performed in Figures 9 and 10, it is clear that even a relatively high measurement uncertainty from the flow instrumentation does not contribute significantly to the combined measurement uncertainty or to the quality of the relative indicators. As the data sheet measurement uncertainty of mass flow instrumentation is considered as a high value, no further attempt is done to quantify the uncertainty of such instrumentation.

Several other factors may contribute in an actual application of the two thermoeconomic diagnosis methods. Therefore, it is difficult to discuss the impact of highly fluctuating load demand and transient operation, like the one often experienced in a commercial refrigeration plant, especially in poorly designed systems where the compressor capacity does not match the different part-load demands [38]. It is expected that unbalanced systems may interfere additionally to the uncertainty of the relative indicator [39]. Such effects may challenge the applicability of thermoeconomic diagnosis. On the other hand, the diagnosis methods will not require a constant full-time monitoring and analysis to evaluate the components, but can be enabled when operation is performing in steady state and relatively close to the design load or reference conditions.

If real steady state observations are not possible to achieve, it may as such be possible to construct a numerical filter to bypass unusable information from the collected data, thus only employ quasistatic measurements in the actual diagnosis procedure. This may on the other hand decrease the quality of the measurements.

Two different measurement uncertainty scenarios are evaluated. The use of the estimated scenario represents the case where the approximation of numerical models allows a simple calibration of the measuring instruments at different reference operating conditions. Using this approach, some of the individual measuring uncertainty contributions, as e.g., linearity deviation and thermal zero point, disappear. This is possible if the characteristic curves and the thermoeconomic models are approximated for a specific refrigeration plant using different measured reference and additional operating conditions data.

A significant choice in the application of the two thermoeconomic diagnosis methods is the choice of the additional operating conditions (and the independent and dependent variables in the characteristic curve method) to model the behaviour of the components, i.e., in terms of the

characteristic curves and the thermoeconomic models for the respective methods under consideration. It is the experience of the authors of this paper, that the selection of the additional operating conditions to accomplish this influences the quality of the diagnosis, although this should intuitively not be the case. Correspondingly it is not certain, that the choice of the additional operating conditions or variables, at the same time yields a satisfactory indication of malfunctions and also a low measurement uncertainty.

In a case where the approximated characteristic curves and thermoeconomic models of the components in one refrigeration system, are applied on another refrigeration system, the measurement uncertainties can possibly be larger than the ones presented by the data sheet measurement uncertainty scenario. This is because the reference operating condition used in the former refrigeration system does not necessarily match the reference operating condition of the second system, as well as the linearity deviation and thermal zero point most likely is changed with a different set of measuring instruments.

5. Conclusions

Two thermoeconomic diagnosis methods were evaluated in terms of their applicability within commercial refrigeration. A common relative indicator for the two methods was proposed, which can be used to directly compare the quality of the identification of intrinsic and induced malfunctions.

Both methods were applicable to evaluate whether a malfunction was intrinsic or induced when using steady state data without measurement uncertainties. The quality of the results was considered equivalent between the two methods. The data supplied to the diagnosis matches the location of already installed measuring instruments, except for the case of flow instruments.

With the introduction of measurement uncertainties, several approaches were possible. In this study the models of the behaviour of the components was calculated based on measured data, with measurement uncertainty. The study was based on two different measurement uncertainty scenarios from the measuring instruments under consideration. Using the data sheet uncertainty scenario, both methods showed overlaps between the relative indicators for components with intrinsic and induced malfunctions due to measurement uncertainties. With the estimated scenario, which represents repeated measurements of fixed instrumentation, both methods were applicable to locate and categorise malfunctions with significant margin between induced and intrinsic malfunctions. For the data sheet uncertainty scenario, a relative indicator above $I_{\mathrm{rel}} = 35$ indicated an intrinsic malfunction in the considered component. Using the estimated uncertainty scenario, the threshold value of the relative indicator for induced effects was $I_{\mathrm{rel}} = 15$ for the characteristic curve method, and $I_{\mathrm{rel}} = 8$ for the thermoeconomic model diagnosis approach.

Both cases were used for an evaluation of the contribution from different measurement instruments using the characteristic curve method. The evaluation showed that the highest contributor of measurement uncertainty from the measuring instrument was component dependent. In the transcritical (HP) compressor unit the most important was the flow measurement instrument, while for the gas cooler the combined contribution of temperature measurement instruments were the most important.

Acknowledgments: The work was supported by the Danish Energy Technology Development and Demonstration programme (EUDP).

Author Contributions: Torben Ommen and Brian Elmegaard conceived and designed the analysis; Torben Ommen created models and performed the calculations; Torben Ommen and Oskar Sigthorsson analysed the data; Torben Ommen, Oskar Sigthorsson and Brian Elmegaard wrote the paper. All authors have read and approved the final manuscript.

Conflicts of Interest: The authors declare no conflict of interest.

Abbreviation

$\dot{E}$	exergy rate, kW
I	indicator, kW
k	unit exergy consumption, /
$\dot{m}$	mass flow, kg/s
p	pressure, kPa
$\dot{Q}$	heat rate, kW
t	temperature, °C
UA	overall conductance in heat exchange, kW/K
$\dot{W}$	power, kW

Greek symbols

Δ	difference or variation from reference state
δ	derivative
η	efficiency
τ	independent thermodynamic variable

Sub- & superscripts

1–11	state point
add	additional operating condition
amb	ambient
calc	calculated
CT	chilled temperature evaporator units
D	destruction
el	electric motor
F	fuel
free	free operating condition
FT	freezing temperature evaporator units
GC	gas cooler unit
HP	high pressure compressor unit
i	component index
k	variable index
LP	low pressure compressor unit
n	operating condition index
m	index for degrees of freedome of component
P	product
rel	relative to exergy destruction rate in reference operating condition
ref	reference operating condition
real	real operating condition
SH	superheat

Appendix A

The reference and real operating conditions of the refrigeration plant, according to the state points defined in Figure 3, are presented in Table A1.

Table A1. The plant data for the reference operating condition and the four operating conditions with malfunctions (Real 1–4).

Variable	Unit	REF	Real 1	Real 2	Real 3	Real 4
t_1	K	270.7	270.5	271.3	270.7	270.4
t_2	K	380.6	380.3	381.5	390.6	383.6
t_3	K	305.6	305.6	305.6	305.6	307.0
t_7	K	272.6	272.6	272.6	272.6	272.6
t_9	K	252.8	252.8	252.8	252.8	252.8
t_{10}	K	304.8	304.8	310.8	304.8	304.8
t_{amb}	K	305.1	305.2	305.2	305.2	305.2
p_1	kPa	2607	2607	2607	2607	2607
p_2	kPa	8651	8652	8651	8652	8945
p_3	kPa	8651	8652	8651	8652	8945
p_4	kPa	3500	3800	3500	3500	3500
p_9	kPa	1409	1409	1409	1409	1409
$\dot{m}_{HP}$	kg/s	0.197	0.197	0.197	0.197	0.202
$\dot{m}_{LP}$	kg/s	0.024	0.025	0.024	0.024	0.024
$\dot{W}_{HP}$	kW	15.4	15.5	15.5	18.0	16.3
$\dot{W}_{HP}$	kW	0.94	0.97	1.10	0.94	0.94

References

1. International Institute of Refrigeration. *The Role of Refrigeration in the Global Economy*; Technical Report; International Institute of Refrigeration: Paris, France, 2015.
2. Verda, V. Thermoeconomic analysis and diagnosis of energy utility systems from diagnosis to prognosis. *Int. J. Thermodyn.* **2004**, *7*, 73–83.
3. Toffolo, A.; Lazzaretto, A. On the thermoeconomic approach to the diagnosis of energy system malfunctions indicators to diagnose malfunctions: Application of a new indicator for the location of causes. *Int. J. Thermodyn.* **2004**, *7*, 41–49.
4. Piacentino, A.; Catrini, P. Assessing the robustness of thermoeconomic diagnosis of fouled evaporators: Sensitivity analysis of the exergetic performance of direct expansion coils. *Entropy* **2016**, *18*, 85.
5. Rossi, T.M.; Braun, J.E. A Statistical, Rule-Based Fault Detection and Diagnostic Method for Vapor Compression Air Conditioners. *HVAC R Res.* **1997**, *3*, 19–37.
6. Tassou, S.A.; Grace, I.N. Fault diagnosis and refrigerant leak detection in vapour compression refrigeration systems. *Int. J. Refrig.* **2005**, *28*, 680–688.
7. Green, T.; Izadi-Zamanabadi, R.; Niemann, H. On the choice of performance assessment criteria and their impact on the overall system performance—The refrigeration system case study. In Proceedings of the 1st Conference on Control and Fault-Tolerant Systems, SysTol'10, Nice, France, 6–8 October 2010; pp. 624–629.
8. Ommen, T.; Elmegaard, B. Numerical model for thermoeconomic diagnosis in commercial transcritical/subcritical booster refrigeration systems. *Energy Convers. Manag.* **2012**, *60*, 161–169.
9. Piacentino, A.; Talamo, M. Critical analysis of conventional thermoeconomic approaches to the diagnosis of multiple faults in air conditioning units: Capabilities, drawbacks and improvement directions. A case study for an air-cooled system with 120 kW capacity. *Int. J. Refrig.* **2013**, *36*, 24–44.
10. Valero, A.; Correas, L.; Lazzaretto, A.; Rangel, V.; Reini, M.; Taccani, R.; Toffolo, A.; Verda, V.; Zaleta, A. Thermoeconomic philosophy applied to the operating analysis and diagnosis of energy utility systems. *Int. J. Thermodyn.* **2004**, *7*, 33–39.
11. D'Accadia, M.D.; de Rossi, F. Thermoeconomic analysis and diagnosis of a refrigeration plant. *Energy Convers. Manag.* **1998**, *39*, 1223–1232.

12. Torres, C.; Valero, A.; Rangel, V.; Zaleta, A. On the cost formation process of the residues. *Energy* **2008**, *33*, 144–152.
13. Piacentino, A.; Cardona, F. Scope-Oriented Thermoeconomic analysis of energy systems. Part I: Looking for a non-postulated cost accounting for the dissipative devices of a vapour compression chiller. Is it feasible? *Appl. Energy* **2010**, *87*, 943–956.
14. Piacentino, A.; Cardona, E. Scope Oriented Thermoeconomic analysis of energy systems. Part II: Formation Structure of Optimality for robust design. *Appl. Energy* **2010**, *87*, 957–970.
15. Agudelo, A.; Valero, A.; Torres, C. Allocation of waste cost in thermoeconomic analysis. *Energy* **2012**, *45*, 634–643.
16. Lourenço, A.; Nebra, S.; Santos, J.; Donatelli, J. Application of an alternative thermoeconomic approach to a two-stage vapour compression refrigeration cascade cycle. *J. Braz. Soc. Mech. Sci. Eng.* **2015**, *37*, 903–913.
17. Lazzaretto, A.; Toffolo, A. A critical review of the thermoeconomic diagnosis methodologies for the location of causes of malfunctions in energy Systems. *J. Energy Resour. Technol. Trans. ASME* **2006**, *128*, 335–341.
18. Toffolo, A.; Lazzaretto, A. A new thermoeconomic method for the location of causes of malfunctions in energy systems. *J. Energy Resour. Technol. Trans. ASME* **2007**, *129*, doi:10.1115/1.2424960.
19. Verda, V.; Serra, L.; Valero, A. A procedure for filtering the induced effects in the thermoeconomic diagnosis of an energy system. In Proceedings of the 2001 ASME International Mechanical Engineering Congress and Exposition, New York, NY, USA, 11–16 November 2001; pp. 447–455.
20. Verda, V.; Serra, L.; Valero, A. Zooming procedure for the thermoeconomic diagnosis of highly complex energy systems. *Int. J. Appl. Thermodyn.* **2002**, *5*, 75–83.
21. Valero, A.; Correas, L.; Zaleta, A.; Lazzaretto, A.; Verda, V.; Reini, M.; Rangel, V. On the thermoeconomic approach to the diagnosis of energy system malfunctions: Part 1: The TADEUS problem. *Energy* **2004**, *29*, 1875–1887.
22. Valero, A.; Correas, L.; Zaleta, A.; Lazzaretto, A.; Verda, V.; Reini, M.; Rangel, V. On the thermoeconomic approach to the diagnosis of energy system malfunctions: Part 2. Malfunction definitions and assessment. *Energy* **2004**, *29*, 1889–1907.
23. Lazzaretto, A.; Toffolo, A.; Reini, M.; Taccani, R.; Zaleta-Aguilar, A.; Rangel-Hernandez, V.; Verda, V. Four approaches compared on the TADEUS (thermoeconomic approach to the diagnosis of energy utility systems) test case. *Energy* **2006**, *31*, 1586–1613.
24. Verda, V.; Borchiellini, R. Exergy method for the diagnosis of energy systems using measured data. *Energy* **2007**, *32*, 490–498.
25. Usón, S.; Valero, A.; Correas, L. Energy efficiency assessment and improvement in energy intensive systems through thermoeconomic diagnosis of the operation. *Appl. Energy* **2010**, *87*, 1989–1995.
26. Silva, J.; Venturini, O.; Lora, E.; Pinho, A.; Santos, J. Thermodynamic information system for diagnosis and prognosis of power plant operation condition. *Energy* **2011**, *36*, 4072–4079.
27. F-Chart Software (LLC.) Available online: http://www.fchart.com/ees/ (accessed on 20 December 2016).
28. Ge, Y.T.; Tassou, S.A. Thermodynamic analysis of transcritical CO2 booster refrigeration systems in supermarket. *Energy Convers. Manag.* **2011**, *52*, 1868–1875.
29. CompSUPER—Produkter til Supermarkeder. Available online: http://www.advansor.dk/produkter/compsuper/ (accessed on 20 December 2016).
30. Bejan, A.; Tsatsaronis, G.; Moran, M. *Thermal Design & Optimization*, 1st ed.; John Wiley & Sons: New York, NY, USA, 1996.
31. Lozano, M.; Valero, A. Theory of the exergetic cost. *Energy* **1993**, *18*, 939–960.
32. Torres, C.; Valero, A.; Serra, L.; Royo, J. Structural theory and thermoeconomic diagnosis: Part I. On malfunction and dysfunction analysis. *Energy Convers. Manag.* **2002**, *43*, 1503–1518.
33. Verda, V. Accuracy level in thermoeconomic diagnosis of energy systems. *Energy* **2006**, *31*, 3248–3260.
34. Danfoss A/S. Data Sheet/Technical Leaflet, AKS 11, PT1000 Temperature Sensor, Superheat Measurement, 2012. Available online: http://sensors.danfoss.com/temperature-sensors/aks11-21/#/ (accessed on 20 December 2016).
35. Danfoss A/S. Data Sheet/Technical Leaflet, AKS 2050, Pressure Transmitter, 2012. Available online: http://sensors.danfoss.com/pressure-transmitters/aks32r-2050/#/ (accessed on 20 December 2016).
36. ABB Inc. Electricity Meters, for Modular Enclosures and DIN Rail, DBB13000, 2010. Available online: http://www.abb.com/product/seitp329/170cfafb1c654c25c125718f002961d6.aspx (accessed on 20 December 2016).

37. Siemens AG. Coriolis Flowmeters, SITRANS F C MASS 2100 Di 3-15, 2013. Available online: http://w3.siemens.com/mcms/sensor-systems/en/process-instrumentation/flow-measurement/coriolis-flow-meter/sensors/pages/sitrans-f-c-mass-2100-di-3-15.aspx (accessed on 20 December 2016).
38. Correas, L. On the thermoeconomic approach to the diagnosis of energy system malfunctions suitability to real-time monitoring. *Int. J. Thermodyn.* **2004**, *7*, 85–94.
39. Zaleta-Aguilar, A.; Domínguez-Vega, R.; Olivares-Arriaga, A.; Rangel-Hernández, V. Thermoeconomic diagnosis theory based on thermo-characterization. *Int. J. Thermodyn.* **2010**, *13*, 143–152.